An Enhanced Canopy Cover Layer for Hydrologic Modeling

CEE 6440: GIS for Water Resources
Term Project

Sara A. Goeking
Submitted 12/02/2016

TABLE OF CONTENTS

Introduction……………………………………………………………………………………………………...2

Study area…….2

Methods………..4

Results……..8

Discussion and future work……………………………………………………………………………….11

Citations………12

ABSTRACT

The purpose of this project was to produce a tree canopy cover layer that can be used as an input to distributed hydrologic models. The canopy cover layer was developed for a test watershed in northwestern Montana using a statistical model, where training data consisted of points representing ground-based measurements of tree canopy cover at permanent forest monitoring plots. Predictor variables represented elevation and topographic derivatives, including hydrologic proximity measures; climate; satellite-based reflectance; soil map units; and existing cover datasets. All predictors were transformed to a common spatial reference system and cell resolution using ArcGIS Pro geoprocessing tools. The output tree canopy cover layer was statistically modeled and validated using empirical Bayesian kriging. The accuracy of the modeled canopy cover layer was evaluated in terms of the mean error and root mean square error (RMSE) of predicted versus observed canopy cover at ground-plot locations. For comparison purposes, these error metrics were compared to those for the National Land Cover Dataset's (NLCD's) 2011 Tree Canopy Cover layer relative to ground-based measurements. Both RMSE and mean error of the modeled tree canopy cover layer were lower than those for the NLCD layer. This result suggests that additional effort may produce an enhanced canopy cover layer at broader scales that may be useful for distributed hydrologic modeling.

INTRODUCTION

Forest cover is included in many hydrologic models because it affects hydrology via canopy interception, evapotranspiration, and effects on snowpack, all of which influence the partitioning of precipitation into runoff versus evapotranspiration. Some models account for canopy resistance and transpiration at multiple canopy levels (e.g., Tague and Band 2004), which means that they can theoretically represent forested watersheds with greater precision than single-level canopy representations. However, the ability of models to incorporate this level of detail is frequently underutilized due to a lack of detailed vegetation data.

Currently most vegetation inputs to distributed hydrologic models consist of either fine-scale vegetation maps for small watersheds, or national-scale maps with coarse attributes. The primary source for data at the latter scale is the National Land Cover Dataset (NLCD), which is updated every 5 years and includes only 3 forest classes: deciduous, evergreen, and mixed (Homer et al. 2015). Simulations of the broad-scale effects of within-class changes, such as fractional decreases in live tree cover due to insect epidemics and/or low- to medium-severity wildfires, are not possible without expansion of the 3 forest classes to a continuous representation of forest cover. The NLCD also includes tree canopy cover (TCC) layers for 2001 and 2011, although documentation warns against comparing multiple temporal TCC layers due to methodological and definitional inconsistencies (Homer et al. 2015).

The existence of a nationwide forest monitoring dataset offers the opportunity to build an enhanced representation of forest cover for hydrologic modeling. The Forest Inventory and Analysis Program (FIA) of the U.S Forest Service has a network of permanent monitoring plots with a mean point spacing of 5 km (Bechtold and Patterson 2005). On each plot, FIA measures vegetation structure including tree cover, tree cover reduction in the previous 10 years, mean tree height, basal area, litter depth, and height and percent cover of understory vegetation by life form. FIA plot locations are based on a probabilistic sampling framework and are re-measured every 5-10 years (Bechtold and Patterson 2005). Therefore, this dataset represents a robust and ongoing source of high-quality cover data for hydrologic modeling purposes.

The goal of this project was to develop a method for statistically modeling a tree canopy cover layer that can be used as an input to distributed hydrologic models. If successful, such an effort could be expanded to a broader geographic area in the U.S., repeated to assess fractional changes in tree canopy cover over time, and possibly modified to produce similar layers for litter and secondary canopy strata.

STUDY AREA

A prototype methodology for creating a tree canopy cover layer was tested in the upper watershed of the South Fork Flathead River, Montana (Fig. 1). The study area is entirely within the Bob Marshall Wilderness Complex and thus is not subject to logging, development, or other changes in land use or land cover that may affect tree canopy cover. It is also upstream from Hungry Horse Reservoir, which represents the upper-most point of flow regulation in this watershed. The upper watershed was delineated and summarized using USGS StreamStats (http://streamstatsags.cr.usgs.gov/streamstats/), a web application from which the watershed boundary was exported as a shapefile. Delineation was based on the location of the USGS gage at Twin Creek near Hungry Horse MT, which has gage ID number 12360000. The watershed covers 1,159 mi^2 (3,001 km^2), with elevations ranging from 3,598 to 9,303 feet. It receives 49.1 inches of annual precipitation and, based on monthly mean evapotranspiration reported by StreamStats, experiences 11.0 inches of evapotranspiration between March and October. Eight-three percent of the upper watershed is forested. It contains 119 permanent forest monitoring plots with canopy cover percentages ranging from 0 to 87.

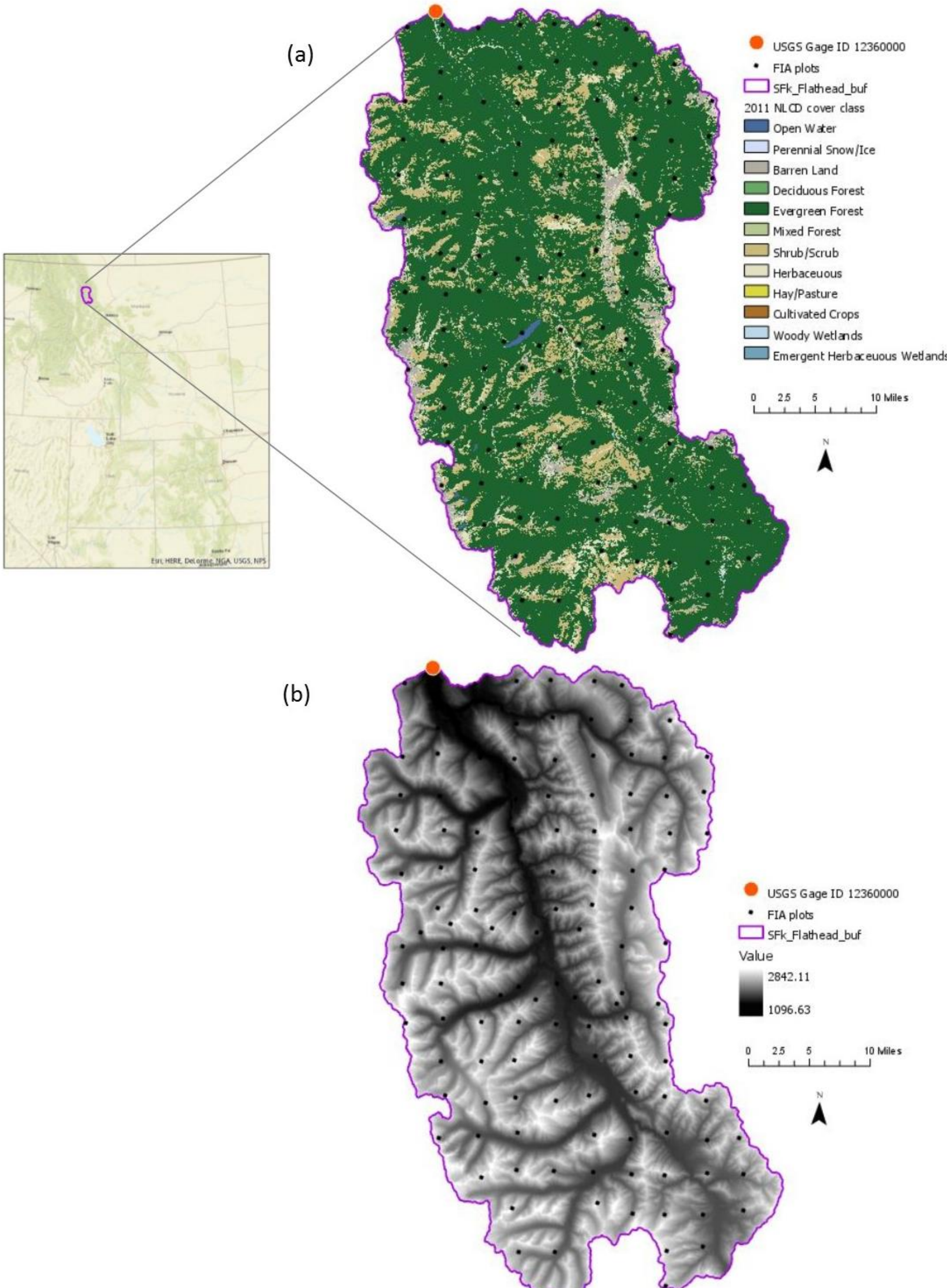

Fig. 1. Study area: The upper South Fork Flathead River watershed in northwestern Montana. Backdrop shows (a) landcover classes, and (b) elevations. Points indicate approximate locations of FIA plots where tree canopy cover was measured.

METHODS

General methods including preparation of response data, processing of predictor data, development of a statistical model of canopy cover, and assessment of the output canopy cover layer. Each of these steps are described in detail below.

The spatial reference system used for this project was the equal-area Albers projection, based on the North American Datum of 1983, with a central meridian of -96.0°, a latitude of origin of 40.0°, first standard parallel of 20.0°, and second standard parallel of 60.0°. All layers that were acquired in other spatial reference systems were transformed to this spatial reference prior to any other processing. To ensure alignment of raster cells among multiple predictor layers, the DEM raster was used as a snap raster in the environment settings for each transformation.

After transformations to get all layers into the Albers NAD83 spatial reference system, layers were clipped to the spatial extent of the study area. Rather than using the topographic boundary of the upper South Fork Flathead River watershed, this boundary was buffered by 100 m to create a new feature class for clipping. The buffered watershed boundary was used to clip predictor layers to avoid edge contamination during topographic analyses.

Response data processing

Response data consisted of tree canopy cover as measured on permanent FIA plots. Tree canopy cover is defined as a vertical projection of tree crowns onto the ground surface (USDA 2013). Values are recorded as percentages from 0 to 100 percent; thus, the canopies of multiple trees are not double-counted, nor are slopes adjusted to provide an oblique estimate of cover. The field procedure for measuring canopy cover consists of several transect-intercept samples per plot, where gaps within the canopy are not counted toward percent canopy cover (USDA 2013). Percent tree canopy cover, geographic plot coordinates, and unique plot identifiers for all plots in eight western states were queried from the national FIA database (O'Connell et al. 2016). The resulting text file was imported to ArcGIS Pro, displayed as XY coordinates, exported to a point feature class, transformed to Albers NAD83, and then clipped to the study area for this project to yield 119 FIA plots (Fig. 1).

Predictor data processing

Table 1 lists the 18 predictor layers and data sources that were used to model canopy cover. Most predictors were downloaded in raster format with 30-m resolution; the two exceptions were the climate and soils datasets (described below). Subsequent processing of each predictor layer is described in more detail here, with each predictor layer in **bold**.

Elevation was represented by a 30-m Digital Elevation Model (DEM). Topographic derivatives included slope, aspect, folded aspect, and heat load index. Fig. 2 shows a workflow for calculating **folded aspect** and **heat load index** in ArcGIS Pro ModelBuilder. **Slope** and aspect were calculated in this model using basic ArcGIS geoprocessing functions, while folded aspect and heat load index were calculated using RasterCalculator. Folded aspect and heat load index were described by McCune and Keon (2002) as a representation of topography that is meaningful for modeling vegetation. Based on calibration against data reported by Buffo et al. (1972), McCune and Keon's (2002) calculations of folded aspect and heat load index assume that heat loading is greatest at aspects facing 225 degrees and lowest at aspects of 45 degrees. Note that these formulations are used to model species distributions (e.g., Evans and Cushman 2009) despite their lack of a strong physical basis with respect to the use of 45- and 225-degree aspects as respective minima and maxima of heat loading. Although the folded aspect used here was based on a datum axis of 45 and 225 degrees, it can also be formulated using 0 and 180 degrees as a datum axis. Both datum axes avoid the problem of representing nearly identical aspects near due north (i.e., 0 or 360 degrees) with a maximum possible difference between values (e.g., 1 versus 359 degrees). Although aspect was used to calculate topographic derivatives, it was not included as a predictor; folded aspect was included instead.

Table 1. List of predictor variables and data sources.

Predictor	Source
Elevation (DEM)	ESRI Data Services
Slope	DEM/ArcGIS Pro function
Folded aspect	DEM/Raster Calculator
Heat load index	DEM/Raster Calculator
Wetness index	DEM/TauDEM
Slope over area ratio	DEM/TauDEM
Distance up to ridge	DEM/TauDEM
Distance down to stream	DEM/TauDEM
LANDSAT 7, Band 2 (blue)	https://landsatlook.usgs.gov/viewer.html
LANDSAT 7, Band 3 (green)	https://landsatlook.usgs.gov/viewer.html
LANDSAT 7, Band 4 (red)	https://landsatlook.usgs.gov/viewer.html
LANDSAT 7, Band 5 (near infrared)	https://landsatlook.usgs.gov/viewer.html
Mean annual precipitation	http://www.prism.oregonstate.edu
Maximum annual temperature	http://www.prism.oregonstate.edu
Minimum annual temperature	http://www.prism.oregonstate.edu
STATSGO soil map units	http://websoilsurvey.nrcs.usda.gov
2011 NLCD cover classes	http://viewer.nationalmap.gov/viewer/
2011 NLCD tree canopy cover	http://geoinfo.msl.mt.gov/

The DEM was also used to calculate several hydrological proximity measures described by Tesfa et al. (2011). These included topographic wetness index, slope over area ratio, distance up to ridge, and distance down to stream. All were calculated using TauDEM functions (Tesfa et al. 2011) in ArcGIS Pro version 1.3. The process of calculating these rasters required a preliminary workflow that is typical for hydrological terrain analyses, which I accomplished with the following TauDEM functions:

1) Pit Remove;
2) D-Infinity Flow Directions; and
3) D-Infinity Contributing Area.

Topographic **wetness index** is calculated as the natural log of A_s/β, where A_s equals the specific catchment area (i.e., the upslope contributing area divided by the width of the grid cell) and β equals the local slope of the grid cell. The TauDEM function for D-Infinity Contributing Area produces A_s in the correct units. Topographic wetness index was originally formulated for modeling the response of a basin to precipitation inputs (Beven and Kirby 1979), and has also been used for modeling vegetation distributions (e.g., Evans and Cushman 2009). The **Slope over area ratio** function in TauDEM is similar to wetness index, but differs in that it calculates the ratio of slope to specific catchment area. Thus it avoids the problem of null values resulting when slope equals zero.

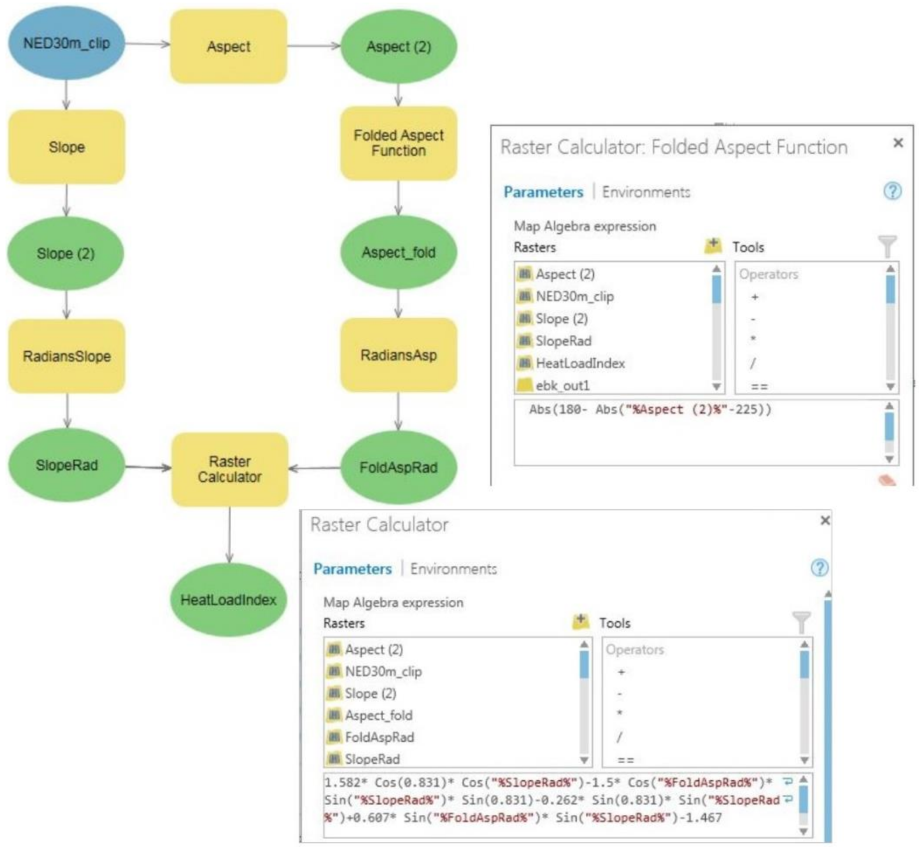

Fig. 2. Structure of the model used to calculate slope, aspect, folded aspect, and heat load index using ArcGIS Pro ModelBuilder. Equations for folded aspect and heat load index from McCune and Keon (2002) are shown in inset boxes and require conversion of slope, aspect, and latitude from degrees to radians.

Distance up to ridge was calculated using TauDEM function “D-infinity distance up”, which follows D-infinity flow paths in a reverse, upward direction to find the nearest ridge cell. **Distance down to stream** was calculated using TauDEM function “D-Infinity distance down”, which follows D-infinity flow paths downward to the nearest stream cell. Because this function requires a stream raster as an input, I used the TauDEM function “Stream definition by threshold” to create a stream raster. The threshold was set at 1,000 cells of contributing area, which produced a stream raster that showed visually good agreement with perennial streams shown on topographic maps and 1-m National Agriculture Imagery Program (NAIP) imagery. Based on my input parameters, the outputs of **Distance up to ridge** and **Distance down** to stream represented the average distances across the surface, rather than minimum or maximum distances of horizontal, vertical, or Pythagorean vectors.

During processing using TauDEM functions, I encountered the following issue when the contributing area function included the option to check for edge contamination: areas known to represent streams had values of “no data” in the specific catchment area raster. Based on TauDEM documentation advising that this check is unnecessary when the DEM has been clipped to a watershed boundary, I re-ran the process without checking for edge contamination. This resulted in a topographically and hydrologically valid output raster for contributing area.

The Landsat 7 ETM+ data used in this project were acquired on July 30, 2015. This date was selected based on three criteria: (1) it is within the growing-season; (2) cloud cover was less than 10% of the study area; and (3) it is available for download without scan lines (i.e., data gaps to the failure of the Landsat 7 scan line corrector have been filled). After downloading the Landsat data for this date, I determined there was no visible cloud cover within the study area. **Landsat bands 2, 3, 4, and 5** were clipped to the study area and projected to Albers NAD83.

Temperature and precipitation data were downloaded from the website for datasets derived using the Parameter-elevation Relationships on Independent Slopes Model, or PRISM (PRISM Climate Group 2012). Three variables were included in the tree canopy cover model: **mean annual precipitation**, **mean minimum temperature**, and **mean maximum temperature**. Each mean value was based on the 30-yr period from 1981 to 2010. The resolution of these datasets was 800 m.

Soil map units were downloaded from the National Resource Conservation Service (NRCS), which has produced two major soil map series in the U.S.: SSURGO and STATSGO. Although SSURGO is higher resolution than STATSGO, it has not been completed for my study area. Therefore, I used **STATSGO soil map units**. They are available in vector format where soil map units are represented by polygons. To prepare soil map units for statistical modeling in ArcGIS Pro, I needed to convert the polygon to a zonal raster. After transformation the vector layer to Albers NAD83, I used the "Polygon to Raster" tool in ArcGIS Pro to create a zonal raster with 30-m resolution with the DEM as a snap raster.

The last two predictors were **2011 NLCD cover classes** and **2011 NLCD tree canopy cover**. The cover map was obtained from the National Map Viewer. Because the nationwide tree canopy cover layer is a very large file, it was downloaded from a GIS data site maintained by the State of Montana (Table 1) where the tree canopy cover layer had already been clipped to the extent of the state.

<u>Statistical analysis and validation</u>

The ArcGIS Pro Geostatistical Analyst function "EBK regression prediction" (EBK stands for empirical Bayesian kriging) was used to create a spatially continuous, 30-m resolution tree canopy cover layer for the upper South Fork Flathead River watershed. The EBK regression prediction function differs from the standard "empirical Bayesian kriging" function in that it can incorporate multiple predictor layers into the model. In other words, the EBK regression prediction function interpolated tree canopy cover based on FIA plots and also on the predictors listed in Table 1. In contrast, the more commonly used empirical Bayesian kriging function would have interpolated tree canopy cover based solely on FIA plots. EBK regression prediction is not available in ArcGIS Desktop and is a new function in ArcGIS Pro.

The EBK regression prediction function includes an internal validation algorithm. Unfortunately the statistical underpinnings of this validation procedure are poorly documented (ESRI 2016). Nonetheless, the output of the interpolation includes not only the tree canopy cover layer, but also layers representing the standard errors of the modeled values, the difference between modeled and observed values at FIA plot locations, and several other diagnostic metrics.

One parameter required for kriging interpolations is the form of the semivariogram, which indicates the degree of spatial correlation among data points. The semivariogram model type was set to exponential, which assumes that spatial autocorrelation diminishes quickly with distance (ESRI 2016), e.g., due to shifts from the north-facing side of a ridgeline that may have dense forest cover to the south-facing side of a ridgeline that may have no forest cover.

To assess the accuracy of the output tree canopy cover layer, I calculated the root mean square error (RMRSE) of model-predicted versus ground-measured tree canopy cover at FIA plot locations. To assess whether this layer represents a potential improvement over the NLCD tree canopy cover layer, I also assessed the RMSE of NLCD canopy cover vs. FIA-measured canopy cover at plot locations, and then compared this RMSE to the RMSE obtained from the EBK regression prediction layer. Additionally, the mean percent tree canopy cover was compared among FIA plots, the EBK-modeled layer, and NLCD layer. Mean FIA-measured tree canopy cover was determined using the Summary Statistics function in ArcGIS Pro, acting on the tree canopy cover field of the attribute table for the point feature class representing FIA plots. Mean EBK-modeled and NLCD tree canopy cover percentages were obtained from the Statistics shown in the Properties of the respective raster layers.

To compare the importance of various predictors, the correlation coefficients of tree canopy cover versus each predictor were calculated by the “cor” function in the open-source statistical software package R. Data were prepared in ArcGIS Pro by using the function “Extract multi values to points” to associated each FIA plot location with all predictor values. The attribute table produced by this function was exported and converted to a comma-separated value file in Microsoft Excel.

RESULTS

Fig. 3 shows the tree canopy cover layer produced EBK regression prediction. This layer had RMSE=16.7%, compared to RMSE=22.8% for the 2011 NLCD tree canopy cover layer relative to FIA plot measurements.

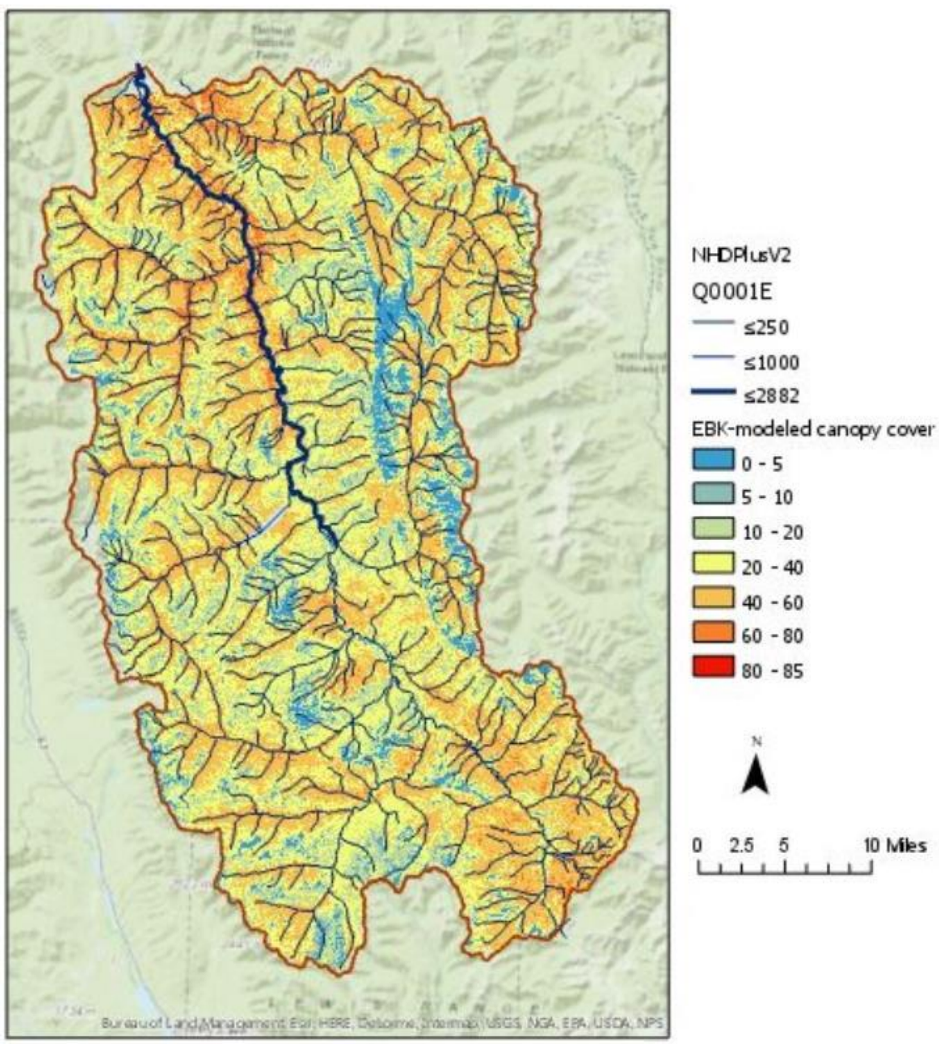

Fig. 3. Map of EBK-modeled tree canopy cover, with NHDPlus flowlines for perspective.

The mean difference between the EBK-modeled and FIA-measured canopy cover was 0.68%, indicating that the modeled layer is not generally biased toward under- or over-estimating tree canopy cover. In contrast, the mean difference between the 2011 NLCD and FIA-measured canopy cover was -13.5%, which represents a general over-estimation of tree canopy cover. Based on these results, the overall accuracy of the EBK-modeled tree canopy cover layer is higher than the 2011 NLCD layer for the upper South Fork Flathead River watershed. The differences between the two canopy cover layers is further illuminated by comparisons of mean canopy cover throughout the watershed. The mean percent tree canopy cover that was measured at 119 FIA plots was 35.7%. The mean cover in the EBK-modeled layer was 34.7%, and the mean of the 2011 NLCD tree canopy cover layer was 46.0%.

Fig. 4 shows the distribution of modeled versus observed canopy cover values at FIA plot locations. This figure further demonstrates that the 2011 NLCD layer over-estimates tree canopy cover compared to EBK regression prediction and ground-based measurements. It also illustrates a limitation of EBK regression prediction: it was not possible to constrain the model to only predict non-negative values. As a result, some negative values of tree canopy cover were predicted; these were truncated to zero in Fig. 3. Therefore, future work to produce an enhanced canopy cover layer should use more flexible multivariate predictive models than EBK regression prediction.

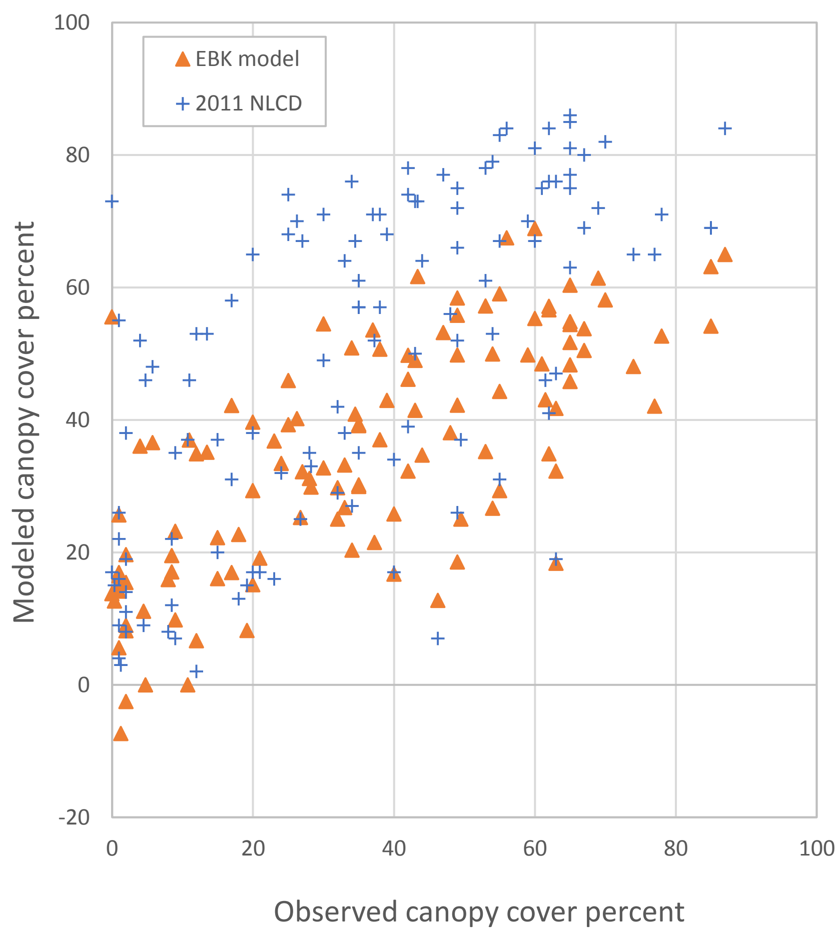

Fig. 4. Scatter plot of modeled versus observed values of canopy cover at FIA plot locations. Modeled values are based on either EBK regression prediction or the 2011 NLCD canopy cover layer. Observed values are based on ground measurements.

Table 2 shows the correlation coefficients of each predictor relative to tree canopy cover. LANDSAT reflectance values (particularly band 5), elevation, distance down to stream, 2011 NLCD canopy cover, temperature, and slope had the highest correlation coefficients. Because the study area has experienced high tree mortality in the past decade due to insects and disease (personal observation, confirmed by FIA plot data), correlation coefficients of predictors versus previous canopy cover are also presented. Most predictors were more strongly correlated with previous canopy cover than with current canopy cover. Thus, it may be important to incorporate predictor layers that represent recent canopy-reducing disturbances, such as data from the Monitoring Trends in Burn Severity (MTBS) program (Eidenshenk et al. 2007) and/or US Forest Service Aerial Detection Surveys (Johnson and Wittwer 2006).

Table 2. Correlation coefficients of predictor variables and tree canopy cover.

	Live canopy cover	Previous canopy cover
Live canopy cover	1.000	0.538
Previous canopy cover	0.538	1.000
Elevation	-0.332	-0.499
Slope	-0.239	-0.388
Folded aspect	-0.032	0.078
Heat load index	-0.030	0.047
Wetness index	-0.024	0.121
Slope over area ratio	-0.085	-0.164
Distance up to ridge	-0.047	0.082
Distance down to stream	-0.294	-0.421
LANDSAT 7, Band 2	-0.322	-0.490
LANDSAT 7, Band 3	-0.364	-0.541
LANDSAT 7, Band 4	-0.255	-0.421
LANDSAT 7, Band 5	-0.450	-0.496
Mean annual precipitation	-0.091	-0.198
Mean annual minimum temperature	0.279	0.411
Mean annual maximum temperature	0.288	0.383
2011 NLCD tree canopy cover	0.665	0.416

One advantage of using EBK regression prediction for this type of modeling is that it produces raster layers representing numerous error metrics. Fig. 5 shows the standard error of the canopy cover map shown in Fig. 3. Such outputs may be useful for exploratory investigation of the nature and distributions of modeling errors. For example, the southern half of the study area appears to have smaller standard errors in predicted canopy cover, compared to the northern half.

Note that both the output tree canopy cover raster and the standard error layer have missing data values along some irregular edges of the study area (Figs. 3 and 5). The locations of missing values suggest that the algorithm uses a bounding box for the kriging analysis, and therefore the corners of the raster used to define the extent should extend beyond the study area.

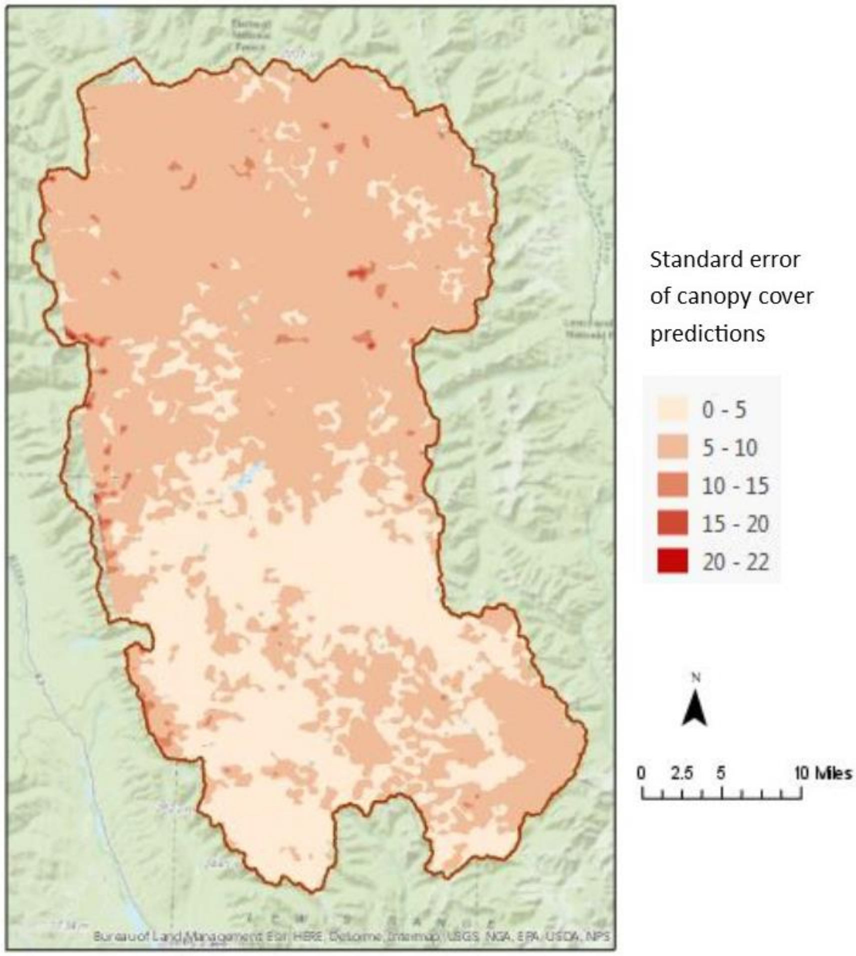

Fig. 5. Map of the standard error EBK-modeled tree canopy cover.

DISCUSSION AND FUTURE WORK

The EBK regression prediction function in ArcGIS Pro seems to be easy-to-use and effective for creating a spatially continuous of canopy cover, provided inputs of multiple raster predictor layers combined with point data representing ground-based canopy cover measurements. The RMSE of the output layer indicated that this method produced a map of tree canopy cover that, for this study area, is more accurate than the 2011 NLCD tree canopy cover layer.

However, this method has some limitations: raster inputs must extend beyond an irregular polygon study area boundary to ensure full coverage in the output layer, and negative predictions cannot be eliminated. For these reasons, the ideal method for developing a statistical model of canopy cover will likely require the use of a more flexible and sophisticated software package, such as the open-source software R.

Based on these the results of this project, it seems worthwhile to pursue additional research into the following aspects of this study:

1) Can the output layer be improved by using a more flexible statistical model?

2) Can additional informative predictors be incorporated?
3) Can this method be repeated across broader geographic scales?
4) Can this method be used to produce similar spatially continuous layers representing secondary canopy strata and litter layers, based on ground measurements at FIA plots?

In reference to the first question, the open-source statistical analysis programming language R offers the greatest flexibility for predictive modeling. Preparing GIS data for analysis in R will require several addition pre-processing steps, some of which were not used here. All data inputs must exist in raster format, with identical spatial reference and cell size. Within R, some functions perform automatic cross-validation. However, the ideal method for validating a modeled layer such as the tree canopy cover map produced here would be using *k*-fold cross-validation, which is considered one of the most efficient, least biased methods of assessing accuracy (Kuhn and Johnson 2013). There is an ample number of FIA plots to permit this type of validation with *k*=5 to 10.

In reference to the second question, the specific predictors that could be improved are topographic derivatives and climate variables. Future work should investigate a more physically-based representation of solar radiation and/or heat load for modeling vegetation. Climatic variables such as precipitation and temperature should be represented at temporally finer scales, such as using individual years or seasons to calculate moving-averages for multiple years or seasons, based on the knowledge that trees may respond to multi-year water or temperature stress (Anderegg et al. 2013). Also, spatial scale is an important consideration for climatic predictors. Although PRISM data are fairly high-resolution at 800 m, statistical modeling in R requires that all inputs have identical cell sizes. Therefore, PRISM data must either be downscaled using an appropriate resampling method, or all other variables must be resampled to 800 m resolution.

This method could theoretically be expanded to broader geographic scales, such as the entire western U.S. If geographic patterns are observed in the error structure of the output canopy cover layer, then it may be necessary to incorporate predictors that provide geographic separation, such as HUC8 watershed or some combination of latitude and longitude, which may be conceptualized as regionally-specific splines in the model.

Finally, the method used here to produce an enhanced canopy cover layer could be repeated in the future as FIA continues re-measurement of permanent plots. That would enable quantification of fractional changes in canopy cover over time, such as those caused by partial mortality during drought, insect epidemics, or low-severity wildfire.

As described in Tague and Band's (2004) description of a spatially distributed hydrologic model, multiple canopy layers and a litter layer can be represented explicitly in their hydrologic model, presumably because those layers affect the rate of infiltration and thus the partitioning of precipitation into evapotranspiration versus runoff. Thus, the capabilities of hydrologic models have exceeded the availability of spatially explicit cover data. Because FIA collects detailed information on multiple canopy strata as well as litter, it is worth investigation whether the methods used here can also produce spatially continuous layers of secondary canopy strata and litter.

CITATIONS

Anderegg, W.R.L.; Plavcová, L.; Anderegg, L.D.L.; Hacke, U.G.; Berry, J.A.; Field, C. B. 2013. Drought's legacy: multiyear hydraulic deterioration underlies widespread aspen forest die-off and portends increased future risk. Global Change Biology 19: 1188–1196. doi:10.1111/gcb.12100

Bechtold, W.A.; Patterson, P.L. [Editors]. 2005. The enhanced forest inventory and analysis program - national sampling design and estimation procedures. Gen. Tech. Rep. SRS-80. Asheville, NC: U.S. Dept. of Agriculture, Forest Service, Southern Research Station. 85 p.

Beven, K.J.; Kirkby, M.J. 1979. A physically based, variable contributing area model of basin hydrology. Hydrologic Science Bulletin 24: 43–69.

Buffo, J.; Fritschen, L.J.; Murphy, J.L. 1972. Direct solar radiation on various slopes from 0 to 60 degrees north latitude. USDA Forest Service Research Paper PNW-142. Portland, OR, US.

Eidenshenk, J.; Schwind, B.; Brewer, K.; Zhu, Z.; Quayle, B.; Howard, S. 2007. A Project for Monitoring Trends in Burn Severity. Fire Ecology Special Issue. Vol. 3, No. 1.

ESRI. 2016. [Online content: http://pro.arcgis.com/en/pro-app/help/analysis/geostatistical-analyst/what-is-ebk-regression-prediction-.htm]. Last accessed 2 Dec 2016.

Evans, J.S; Cushman, S.A. 2009. Gradient modeling of conifer species using random forests. Landscape Ecology 2009: 673-683.

Homer, C.G., Dewitz, J.A., Yang, L., Jin, S., Danielson, P., Xian, G., Coulston, J., Herold, N.D., Wickham, J.D., and Megown, K. 2015. Completion of the 2011 National Land Cover Database for the conterminous United States-Representing a decade of land cover change information. Photogrammetric Engineering and Remote Sensing, v. 81, no. 5, p. 345-354.

Johnson, E. W.; Wittwer, D. 2006. Aerial detection surveys in the United States. In: Aguirre-Bravo, C.; Pellicane, Patrick J.; Burns, Denver P.; and Draggan, Sidney, Eds. 2006. Monitoring Science and Technology Symposium: Unifying Knowledge for Sustainability in the Western Hemisphere Proceedings RMRS-P-42CD. Fort Collins, CO: U.S. Department of Agriculture, Forest Service, Rocky Mountain Research Station. p. 809-811.

Kuhn, M.; Johnson, K. 2013. Applied predictive modeling. New York, NY: Springer. 600 p.

McCune, B.; Keon, D. 2002. Equations for potential annual direct incident radiation and heat load. Journal of Vegetation Science 13:603-606.

O'Connell, B.M.; Conkling, B.L.; Wilson, A.M.; Burrill, E.A.; Turner, J.A.; Pugh, S.A.; Christiansen, G.; Ridley, T.; Menlove, J. 2016. The Forest Inventory and Analysis Database: Database description and user guide version 6.1.1 for Phase 2. U.S. Department of Agriculture, Forest Service. 870 p. Available online: http://www.fia.fs.fed.us/library/database-documentation/current/ver611/FIADB%20User%20Guide%20P2_6-1-1_final.pdf; last accessed 18 October 2016.

PRISM Climate Group, Oregon State University, http://prism.oregonstate.edu, created 1 July 2012.

Tague, C., and Band, L.E., 2004. RHESSys: Regional Hydro-Ecologic Simulation System—an object-oriented approach to spatially distributed modeling of carbon, water, and nutrient cycling. Earth Interact 8(19): 1–42.

Tesfa, T.K.; Tarboton, D.G.; Watson, D.W.; Schreuders, K.A.T.; Baker, M.E.; Wallace, R.M. 2011. Extraction of hydrological proximity measures from DEMs using parallel processing. Environmental Modelling & Software 26: 1696-1709.

U.S. Department of Agriculture, Forest Service. 2013. Interior West Forest Inventory and Analysis Forest Survey field procedures, Ver. 5.0. Available online: http://www.fs.fed.us/rm/ogden/data-collection/pdf/iwfia_p2_60.pdf; last accessed 18 October 2016.